

Effect of Geogrid Geometry on Interface Resistance in a Pullout Test

Jongwan Eun¹, Ph.D., P.E.; Ranjiv Gupta², Ph.D., P.E.; Jorge G. Zornberg³, Ph.D., P.E.

¹Assistant Professor, Univ. of Nebraska-Lincoln, Lincoln, NE. E-mail: jeun2@unl.edu

²Project Engineer, Geosyntec Consultants, Phoenix, AZ. E-mail: rgupta@geosyntec.com

³Professor and W. J. Murray, Jr. Fellow in Engineering, Civil, Architectural & Environmental Engineering, Univ. of Texas at Austin, Austin, TX. E-mail: zornberg@mail.utexas.edu

Abstract

This paper presents the effect of aperture size on the low displacement stiffness response of geogrids subjected to pullout loading. The aperture size of geogrid was varied by cutting ribs of geogrids in the pullout tests. Two types of geogrids were tested at two normal pressures (21 kPa and 35 kPa). The Soil-Geosynthetic Composite (SGC) model was used to compute the low displacement interface stiffness (K_{SGC}) of the geogrids. Based on the analysis of laboratory tests using SGC model, the results showed response of geogrids was highly dependent on the aperture size. The geogrid with original aperture size showed the highest K_{SGC} value. As the size of the aperture increased, the K_{SGC} decreased possibly due to reduction in the passive resistance of transverse members and the loss of confinement at the junctions of the geogrid.

INTRODUCTION

Geogrids have been widely used in stabilization of pavements for several decades. The performance of reinforced flexible pavements is governed by the interaction mechanisms between soil and geosynthetic. The interaction of the geogrid with surrounding soils consists of the passive resistance due to the thickness of rib, the friction of the surface of rib and the confinement of soil in the aperture due to the rib. Generally, the interaction developed between the soil and the reinforcement is a function of soil type, reinforcement type and how they are linked with each other (Teixeira et al. 2007). Actually, these factors are interrelated, and the combined effect of these factors results in complex interactions. Hence, appropriate laboratory test incorporating these variables should be to quantify the interaction mechanisms between the soil and the reinforcement.

Previous studies have focused on investigating the performance of geogrid reinforcement in flexible pavements using laboratory confined tests (Sugimoto et al. 2001, Palmeira 2004, Bergado et al. 2008), because they can provide: (a) the ability to capture the mechanism of lateral restraint; (b) parameters for mechanistic-empirical design; (c) repeatability of test results; (d) a parameter that distinguishes between the performance of various geosynthetics; (e) sensitivity to low displacement

magnitudes; and (f) convenience to conduct in the laboratory. Based on these advantages, a pullout test in a confined soil with monotonic loading has been used to reduce the variability in test results and to allow for the realistic measurement of the interface mechanisms.

The geogrid geometry is a significant factor influencing pullout behavior of geogrid embedded in soils. Geogrid with comparatively large apertures, unlike other reinforcements (e.g. geotextiles) can sustain outer loading by providing both passive and frictional resistance components by transverse and longitudinal members (Teixeira et al. 2007, and Palmeira et al. 2004, 2008). Stress distribution between transverse and longitudinal members of the geogrid is affected by the geogrid geometry. However, there is much uncertainty about the complex influence of geogrid geometry.

This research evaluated the effect of the geogrid geometry associated with various factors on the pullout behavior by using pullout stiffness at the interface between the geogrid and soil. The Soil-Geosynthetic Composite (SGC) model was used to illustrate analytically the interfacial mechanism governing reinforced soil with geogrid. The interface stiffness (K_{SGC}) obtained from the model was evaluated to quantify the effect of the geogrid. A series of pullout tests was conducted to examine the pullout behavior of the geogrid in a confined soil and to determine the stiffness. Based on the results, the combined effects of the geogrid geometry associated with the type of the reinforcement, the confining pressure on the specimen, and the orientation of the specimen on the pullout behavior were investigated.

SOIL-GEOSYNTHETIC COMPOSITE (SGC) MODEL

Geosynthetic load-strain relationship. A load-transfer mechanism of geosynthetic in a confined soil demands to properly simulate the shear stress generated at the interface between the geosynthetic and the soil. To model the mechanism, an infinitesimal geosynthetic element subjected to force (F) in the pullout direction and to the shear stresses (τ) along both surfaces of the geosynthetic element of length (dx) surrounded soil mass can be assumed (Figure 1). Then, the force equilibrium can be given in differential form as follows:

$$F(x) - \{ F(x) - dF(x) \} = 2\tau(x)dx \quad (1)$$

$$\tau(x) = \frac{1}{2} \frac{dF(x)}{dx} \quad (2)$$

On the other hand, assuming that strain $\varepsilon(x)$ develops in the dx due to the change in confined force between two points in the element, the confined force and strain are related through confined stiffness (J_c) of the geosynthetic and is given as:

$$F(x) = J_c \cdot \varepsilon(x) = J_c \frac{dw(x)}{dx} \quad (3)$$

Because the strain developed in the dx can then be related, the F can be described as a differential form.

$$\frac{dF(x)}{dx} = J_c \frac{d\varepsilon(x)}{dx} = J_c \frac{d^2w(x)}{dx^2} \quad (4)$$

Substituting Eq. 4 into Eq. 2 gives,

$$\tau(x) = \frac{1}{2} \frac{dF(x)}{dx} = \frac{1}{2} J_c \frac{d^2w(x)}{dx^2} \quad (5)$$

The above expression is a second-order differential equation governing the soil-geosynthetic interface behavior during the pullout test (Gupta 2009, Zornberg et al. 2009). The equation associates the displacement, $w(x)$ with the $\tau(x)$ developed at the soil-geosynthetic interface in terms of confined stiffness J_c , for the geosynthetic element of length dx in the pullout test (Gupta 2009, Zornberg et al. 2009).

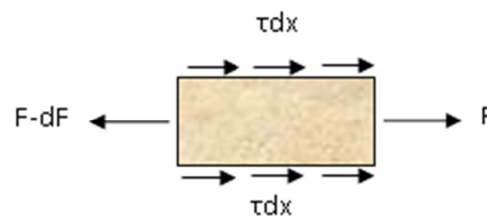


Figure 1. Free body diagrams for geosynthetic element of length dx in pullout test.

Interface stiffness (K_{SGC}). The Soil-Geosynthetic Composite (SGC) model was proposed to describe the relationship between the confined force and the displacement at the soil-geosynthetic interface (Gupta 2009). As substituting Eq. 5 into Eq. 3 with the assumption of the constant shear stress along the geosynthetic element, the force at x was obtained as follow.

$$F(x) = J_c \frac{dw(x)}{dx} = J_c \left(\frac{2\tau_y}{J_c} x + C_1 \right) \quad (6)$$

If the second partial derivative equation, Eq. 5 is solved, the $w(x)$ is given,

$$w(x) = \frac{\tau_y}{J_c} x^2 + C_1 x + C_2 = \frac{F(x)^2}{4\tau_y J_c} \quad (7)$$

where τ_y is the yield shear stress. The τ_y is consistent at a point along the confined length of geosynthetic and independent of the displacement. C_1 and C_2 are constant parameters determined by solving the second derivative equation with the initial and boundary condition in the test (Gupta 2009, Zornberg et al. 2009). The $w(x)$ is equal to the right term of Eq. 7 as incorporating the given constants and conditions. More detailed derivation and the determination of the parameter was described and validated in Gupta (2009).

To realistically capture the interactions developed between soil and geosynthetic at low displacement magnitudes, it is necessary to compute force where the displacements are being measured during the pullout test. Eqs. 6 and 7 can be

used to determine the response of geosynthetic for given displacement increment. This can then be translated to quantify the soil-geosynthetic response to obtaining a measurement for a lateral restraint mechanism developed in the reinforced flexible pavements by using pullout test data. Thus, the equations were solved to obtain the relation between confined force and displacement in terms of model parameters as shown below.

$$F(x)^2 = (4\tau_y \cdot J_c) \cdot w(x) = K_{SGI} \cdot w(x) \quad (8)$$

The force and displacement at any given point x throughout the geosynthetic can be related by model parameters i.e., the yield shear stress (τ_y) and confined stiffness (J_c) of the soil-geosynthetic system. A coefficient of interface stiffness (K_{SGI}) enables to evaluate soil-geosynthetic interaction (Gupta 2009, Zornberg et al. 2009).

MATERIALS AND METHODS

Geogrid. Two different geogrid products, GG1 and GG2 were used as a reinforcement for the pullout test series (Figure 2). GG1 is comprised of knitted polypropylene (PP) yarns, crafted into a stable, interlocking pattern, and then coated for protection from installation damage. On the other hand, GG2 is an integrally formed, punched-and-drawn polypropylene (PP) grid featuring raised protrusions at each rib intersection to provide a structural abutment when placed between soil layers. The properties of GG1 and GG2 were listed in Table 1. The geogrids were prepared with dimensions of 0.6 m length and 0.45 m width for pullout test (ASTM D6706). Four different geometries—the original geogrid, the geogrid with only half of the transverse members, the geogrid with a doubled opening size and the geogrid with only longitudinal members—were used in this study. The designated specimen was prepared by cutting transverse members using pliers. The GG2 with half transverse members was not tested due to its large aperture size.

LVDT. Five LVDTs were used to measure displacements at locations with a horizontal spacing of 100, 200, 300, 450, and 600 mm from the front end of the specimen, named LVDT 1 to 5. The displacement profile throughout the length of the geogrid could be monitored by installing LVDTs at various locations. The displacement rate of testing was set to 1mm/min, (ASTM D6706). The displacement of the specimen occurred as the specimen started to move due to pullout force.

Soil. Monterey No. 30 sand was used as the backfill material for pullout testing. Monterey No. 30 sand is a clean and poorly graded, which was classified as SP according to the Unified Soil Classification System (USCS) (Zornberg et al. 1998). The test was conducted at the relative density of 50%.

Pullout test. The pullout test equipment consisted of a steel box (1.5 m × 0.6 m × 0.3 m), reaction frame, and applying pullout system (Figure 3a). The front end of the box had an opening of 50 mm and had two sleeves of 75 mm length to minimize the influence of the frontal box wall on pullout test results. In the front of the pullout box, the roller grips and its support trolley were designed to avoid stress concentration at

the geosynthetic reinforcement. In the pullout box, the steel plates were used as the reaction frame system with wooden boards (Figure 3b). Six air cylinders were used for applying normal pressure on the surface of soils. The reaction frame system is a reliable way to apply a constant confining pressure on top of the geosynthetic specimen. Two hydraulic pistons were attached to the both side of the pullout box to apply pullout force on the specimen. The electric pump enabled better control over the rate of testing, since it could be independently controlled using the flow valve attached to it. The displacement transducers were attached to the system enabling faster data acquisition.

Table 1. Properties of geogrids used in the study.

Property	Test method	Units	GG1	GG2
Rib shape	Observation	-	Rectangular	Rectangular
Rib Thickness	Calipers	mm	0.5	0.76
Norminal Aperture size	Calipers	mm	15 × 15	25 × 33
Junction efficiency	GRI-GG2-87	%	-	93
Flexural Rigidity	ASTM D1388-96	mg-cm	100,000	250,000
Aperture Stability modulus	Kinney (2001)	m-N/deg	0.44	0.32
Minimum true initial modulus	ASTM D6637-01	kN/m	250	250
MD		kN/m	350	400
XD				
Tensile strength at 2% strain	ASTM D6637-01	kN/m	5	4.1
MD		kN/m	7	6.6
XD				

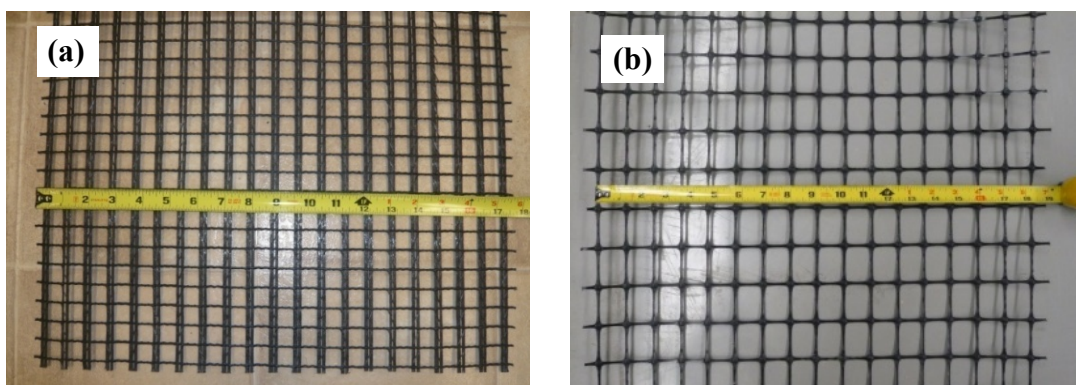


Figure 2. Geogrid used for a pullout test: (a) GG1; and (b) GG2.

A total of thirteen pullout tests were conducted which were grouped into three main series: 1) type of geogrid; 2) confining pressure; and 3) orientation of specimen. All three series includes tests conducted with varying geometry of geogrid.

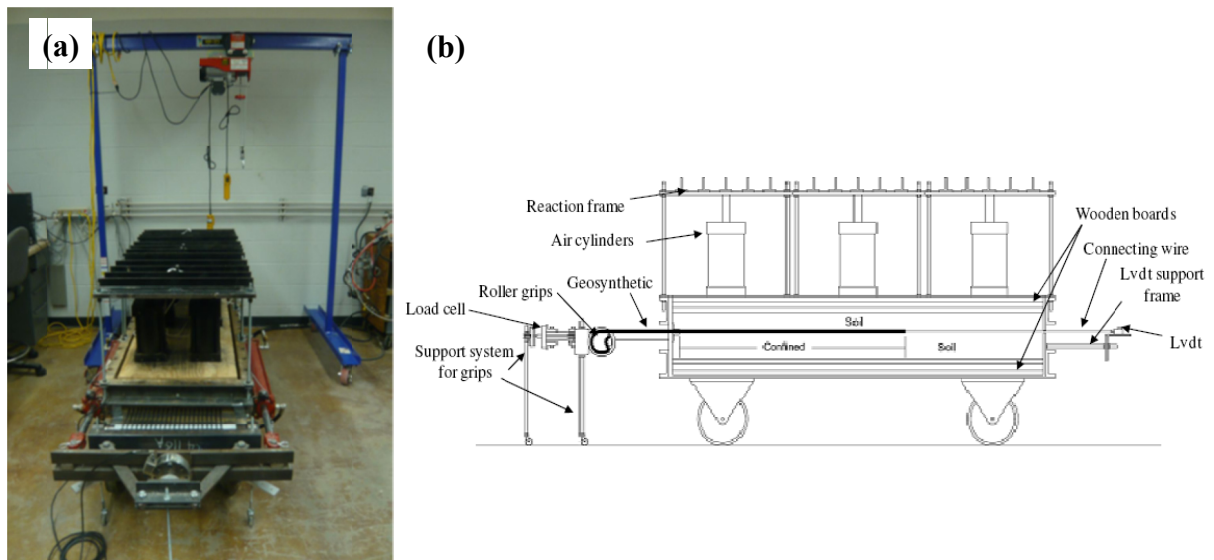


Figure 3. Schematic of pullout testing equipment: (a) photo of testing equipment; (b) side view.

PULLOUT BEHAVIOR OF GEOGRID IN CONFINED SOIL

Figure 4a shows the frontal pullout force of the original GG2 (without altering the apertures) and the displacement obtained at each LVDT with increasing time. The recording of the values was started after the setup time. The force increased gradually with increasing time. The displacement of LVDT 1 located at the front of the geogrid occurred first, and the increasing rate of the displacement was the highest. Likewise, the displacement of LVDT 5 located at the end occurred lastly, and the rate was the lowest. Accordingly, the displacement of the LVDTs and the increasing rate of the displacement were dependent on the locations. The displacement of LVDT placed closer to the front of the pullout box was triggered first. The pullout force increased rapidly at the initial time, but the increasing rate of the force would decrease markedly till approaching the failure (the displacement > 15 mm). After finishing the test, the data was analyzed to obtain the confined force, $F(x)$ and displacement, $w(x)$ at certain point x along the reinforcement proposed in the SGC model [see Figure 1 and Eq. (1) to (8)] (Gupta 2009, Zornberg et al. 2009).

Figure 4b shows the typical development of pullout forces in the front of pullout box versus the displacement at each LVDT during the pullout testing. The reason why the results fluctuated is because slippage between soil and geogrid occurred during the test. As the displacement at each LVDT increased, the frontal pullout force also increased, because the resistance of the interface between the soil and the geogrid started to be generated. Similar to Figure 4a, the displacement at LVDT 1 is the highest. The initial pullout force increased rapidly and approached the

plateau after the peak. The increasing amount of frontal pullout force significantly decreased with increasing the displacement. The maximum pullout force value for the given test was 15.5 kN/m.

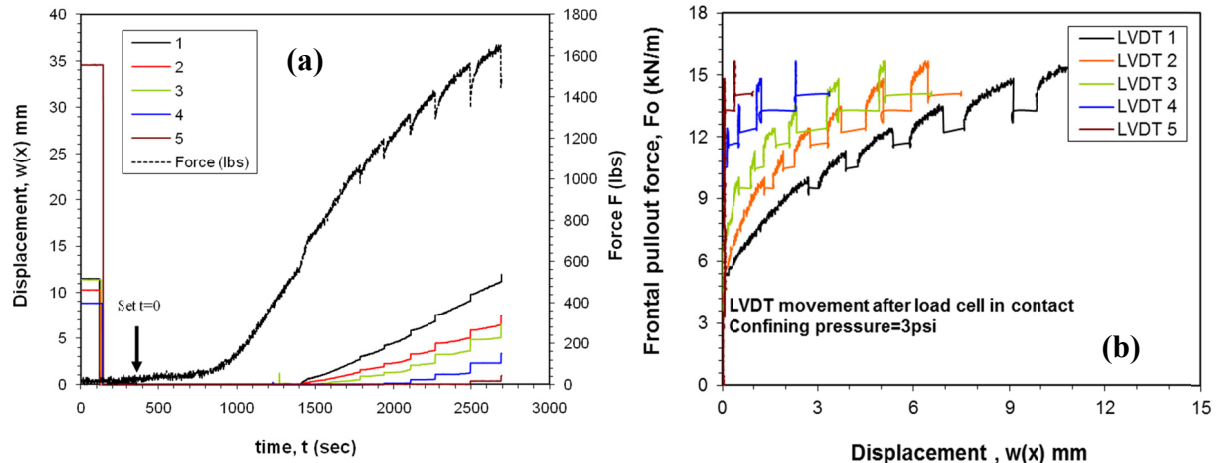


Figure 4. Frontal pullout force and displacement curve for each LVDT: (a) as function of time from the start of test; (b) force vs. displacement curves

PULLOUT BEHAVIOR FOR DIFFERENT GEOMETRIES, GEOGRID TYPE, CONFINING PRESSURE, AND ORIENTATIONS OF GEOGRID

Figure 5a presents the comparison of the frontal pullout force with time obtained using GG1 with various geometries at LVDT 2 with time. The pullout force of the original geogrid without altering the geometry and the half transverse members are the highest value among three cases. The force of GG1 with half transverse members was similar to that of the original GG1 because both the friction and the bearing members that made up the geogrid were not eliminated by removing half transverse members. Significant reduction of the pullout resistance was observed for the GG1 with double aperture and only longitudinal members. In Figure 5b, the frontal pullout force with time obtained using GG1 and GG2 at LVDT 2 was compared. Although the tensile strength of two geogrids was very similar under unconfined condition, the pullout resistance did not show similar results. The pullout force of the GG1 increased much faster than that of GG2. The ultimate pullout strength was not shown clearly, but the overall pullout force obtained for GG1 was higher than that obtained for GG2. The confinement of the GG1 might be higher due to having more ribs and less aperture size than that of the original GG1. Figure 5c shows the comparison of the frontal pullout force of the GG1 under two different confining pressures (21 and 35 kPa) at LVDT 2 with displacement. Unfortunately, the test results for double aperture in the high confining pressure was not obtained, because the specimen was broken before the displacement occurred. The pullout force under high confining pressure was much higher than that under low confining pressure. The effect of the geogrid geometry was significantly subjected to the high pressure. The pullout force in both cases dropped remarkably with changing the geometry. In Figure 5d, the

frontal pullout force with time using a different orientation of the GG2 was compared. Although the properties of transverse and longitudinal members are identical, the pullout resistance according to the orientation of the specimen does not show identical results, because the stress was distributed differently according to the aperture shape of the specimen. In the case of using original specimen, the pullout force in the machine direction (MD) is slightly higher than that in the cross machine direction (XD). However, the pullout force of the XD becomes higher than that of the MD in the case using the geogrid including double aperture and only longitudinal members. The reason is due to the confinement of the soil in the square aperture of the specimen.

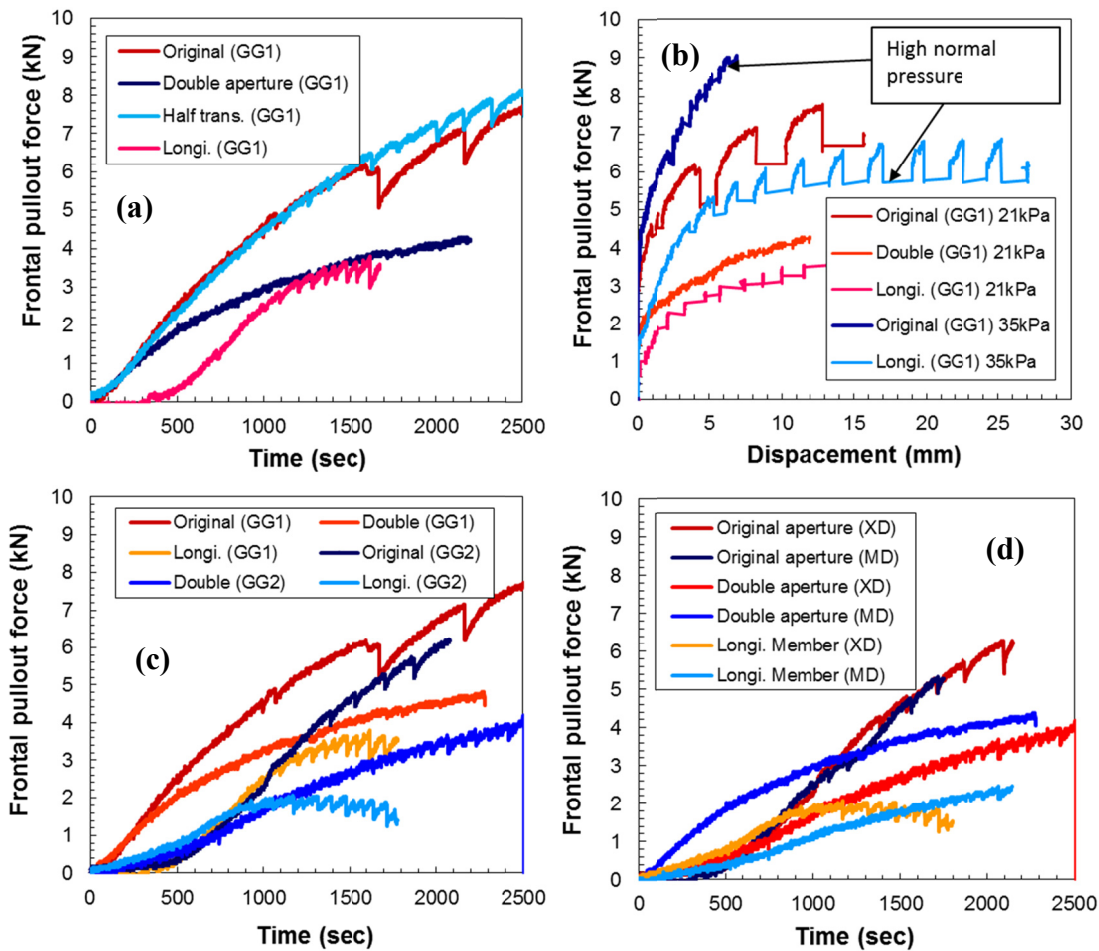


Figure 5. Comparison of frontal pullout force curves for: (a) different geometry (aperture) of GG1 (b) geogrid type of GG1 and GG2; (c) different confining pressure of 21 and 35 kPa; and (d) different orientation of GG2 for MD and XD.

PULLOUT BEHAVIOR AT SMALL DISPLACEMENT RANGE

In the SGC model, an interface stiffness parameter (K_{SGC}) to quantify soil-geosynthetic interaction was defined at low displacement (< 2.5 mm). The K_{SGC} can be obtained from a slope in the plot of the relationship between the squared confined force (Eq. 8) and displacement as shown in Figure 6. The slope can be computed

from the regression analysis with least square method. The increasing rate of the frontal pullout forces (Figure 5c) decreased with increasing displacement. However, the plot of K_{SGC} shows a relatively linear slope within 2.5 mm. To quantify the effect of geogrid geometry on pullout behavior as well as other factors such as the confining pressure on the specimen, the geogrid orientation, and the geogrid type, the pullout testing data in all cases were interpreted.

Effect of geogrid geometry and geogrid type. Figure 5a compared the K_{SGC} obtained for GG1 and GG2 with the original without altering the aperture and the longitudinal only members. The slope of the GG1 is stiffer than that of the GG2 in all cases involving different geometries. The K_{SGC} obtained for GG1 for the original geogrid is higher than that obtained for GG2 by approximately 50%. However, in the only longitudinal members, the value of K_{SGC} of GG1 is around six times higher than that of GG2. GG1 has stronger longitudinal members than transverse members, so the pullout force distributes more to the longitudinal members in GG1 than GG2.

Effect of geogrid geometry and confining pressure. Figure 6b shows the comparison of K_{SGI} under different confining pressure such as 21 and 35 kPa. The K_{SGC} in high confining pressure was higher than that in low confining pressure. The difference of K_{SGC} between high and low confining pressure was much larger in the case of the original geogrid without altering the aperture than that in the case of the geogrid including longitudinal only members. This was because the confinement due to the ribs is applied strongly when the transverse members are present. From these results, the effect of transverse member contributes much more to total pullout resistance when comparatively high confining pressure is applied to the geogrid.

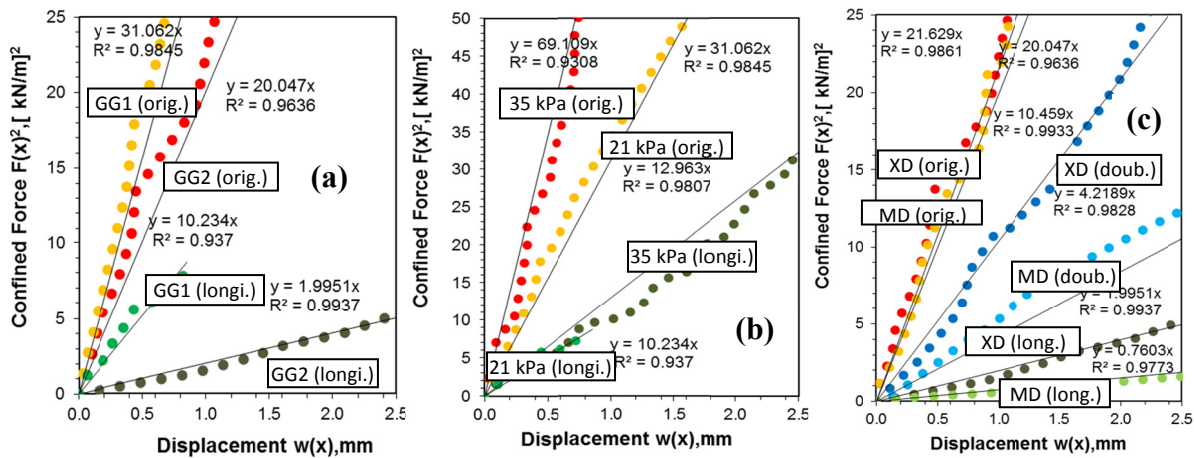


Figure 6. Comparison of K_{SGC} of different geogrid geometry: (a) the geogrid type between GG1 and GG2 in 21 kPa of confining pressure; (b) the confining pressure between 21 and 35 kPa of GG1; and (c) the orientation of GG2 between MD and XD in 21 kPa of confining pressure.

Effect of geogrid geometry and geogrid orientation. Figure 6c shows the comparison of K_{SGC} for different orientation of geogrid combined with the geometry of both the original and the double aperture size. The GG2 was tested under 21 kPa of

confining pressure. The area of transverse ribs in the original case without altering the aperture was increased if the specimen was tested in the MD instead of the XD. However, as the number of transverse member decreases and the area of aperture increases in other cases to control the geometry, the values of K_{SGC} are reduced rapidly in the MD, because the confinement due to transverse members for passive resistance is less than in the XD. As in the previous case, the confinement due to ribs was found to strongly influence the K_{SGC} .

CONCLUSIONS

This paper presents the effect of geogrid geometry, geogrid type, confining pressure, and geogrid orientation on the pullout behavior of geogrid reinforced soil. Based on results of a series of pullout tests, the interface stiffness (K_{SGC}) was evaluated at small displacement range (< 2.5 mm). The value of K_{SGC} was found to decrease with increasing aperture size of the geogrid specimen. This was to the reduction in the passive resistance of transverse members of the geogrid and loss of confinement at the junctions. The difference of K_{SGC} between high and low confining pressure was much larger in the case of the original geogrid than that in the case of the geogrid with only longitudinal member. The values of K_{SGC} are reduced rapidly in the MD because the confinement due to transverse members for passive resistance is less than in the XD. Based on the results obtained in this study, it was found that geogrid geometry strongly influences the pullout behavior of geogrids under small displacements.

REFERENCES

- Bergado, D.T., Teerawattanasuk, C., (2008), "2D and 3D numerical simulations of reinforced embankments on soft ground", *Geotextiles and Geomembranes* Vol. 26, No.1, pp 39–55.
- Gupta, Ranjiv, (2009), "A Study of Geosynthetic Reinforced Flexible Pavement System", Ph.D. Dissertation, the University of Texas at Austin, Texas, USA.
- Li, C., (2005), "Mechanical Response of Fiber-Reinforced Soil", Ph.D. Dissertation, the University of Texas at Austin, Texas, USA.
- Sugimoto, M., Alagiyawanna, A.N.M. and Kadoguchi, K. (2001), "Influence of rigid and flexible face on geogrid pullout tests", *Geotextiles and Geomembranes*, Vol. 19, No.5, 257-277.
- Palmeira, E.M. (2004), "Bearing force mobilization in pullout tests on geogrids", *Geotextiles and Geomembranes*, Vol. 22, No.6, pp 481-509.
- Palmeira, E.M. (2008), "Soil-geosynthetic interaction: Modeling and Analysis", Mercer Lecture, presented at 4th European Conference on Geosynthetics-EuroGeo4, Edinburgh 2008.
- Teixeira, S.H.C., Bueno, B.S. and Zornberg, J.G., (2007), "Pullout Resistance of Individual Longitudinal and Transverse Geogrid Ribs", *Journal of Geotechnical and Geoenvironmental Engineering*, Vol. 133, No. 1, January 1, 2007, pp. 37-50.

- Zornberg, J.G., Ferreira, J.A.Z., Gupta, R.V., Joshi, R.V., and Roodi, G.H. (2009). Geosynthetic-Reinforced Unbound Base Courses: Quantification of the Reinforcement Benefits. Center for Transportation Research (CTR), Report No. FHWA/TX-10/5-4829-1, Austin, Texas, December 2009, Revised February 2012, 170 p.
- Zornberg, J.G., Sitar, N., and Mitchell, J.K. (1998). "Limit Equilibrium as Basis for Design of Geosynthetic Reinforced Slopes." *Journal of Geotechnical and Geoenvironmental Engineering*, ASCE, Vol. 124, No. 8, pp. 684-698.